International Journal of Current Research and Modern Education (IJCRME)
Impact Factor: 6.925, ISSN (Online): 2455 - 5428
(www.rdmodernresearch.com) Volume 3, Issue 1, 2018

EFFECT OF N-DOPING ON STRUCTURAL AND OPTICAL PROPERTIES OF TiO_2 NANOCRYSTALS

G. D. Gena*, T. H. Freeda & K. Monikanda Prabu***

* Physics Research Centre, S.T Hindu College, Affiliated to Manonmaniam Sundaranar University, Tirunelveli, Nagercoil, Tamilnadu

** Department of Physics, S.T Hindu College, Affiliated to Manonmaniam Sundaranar University, Tirunelveli, Nagercoil, Tamilnadu

Cite This Article: G. D. Gena, T. H. Freeda & K. Monikanda Prabu, "Effect of N-Doping on Structural and Optical Properties of TiO_2 Nanocrystals", International Journal of Current Research and Modern Education, Volume 3, Issue 1, Page Number 464-467, 2018

Abstract:

Nanocrystalline anatase phase N-doped TiO_2 nanocrystals are synthesized by Sol-Gel method. The TiO_2 nanocrystals are prepared from the reaction of Titanium (IV) isopropoxide, ethyl alcohol, and H_2O. The crystalline phase is observed from powder X-ray diffraction (PXRD) pattern. PXRD measurements prove the exclusive presence of the anatase phase. Fourier transform infrared spectroscopy (FTIR) is investigated in order to confirm the vibrations of N-H bond in the N-doped TiO_2 crystal lattice, which is found at 3393 cm^{-1}. The optical band gap value of N-doped TiO_2 nanocrystals are estimated from Tauc's plot.

Key Words: Anatase TiO_2, Sol-Gel Method, FTIR, Tauc Plot

1. Introduction:

Titanium dioxide (TiO_2) is a nontoxic, relatively inexpensive oxide compound and the well-known phase is anatase. TiO_2 is used in the preparation of many composites [1, 2], self-cleaning [3, 4] and bactericide [5, 6] materials. This material is considered as a wide bandgap oxide semiconductor with the energy gap of 3.2eV. Among the various semiconductor, TiO_2 demonstrates the highest photocatalytic efficiency due to its appropriate location of energy band, relatively high adsorption affinity towards organic molecules [7-13]. An effective way to extend the absorption of TiO_2 from UV to the visible region is doped with non-metal atoms. Sol-gel is one of the most exploited techniques, which is used to produce thin films and powder Nanocrystals. In this paper, attempt to made synthesis N-doped powder TiO_2 nanocrystals by Sol-Gel method at room temperature, and the structural and optical characterization results are analysed.

2. Synthesis of TiO_2 Nanocrystals:

TiO_2 nanocrystals are prepared via Sol-Gel method using the precursor Titanium (IV) isopropoxide (TTIP, 97%, Sigma Aldrich), deionised water and ethyl alcohol. In this procedure, 100 ml of ethyl alcohol is added to 15 ml of TTIP in a beaker. The pH of the above solution is achieved to acidity range using acetic acid. Then the mixed solution is stirred 10 minutes using magnetic stirrer. 10 ml of deionised water which contains a suitable amount of urea (Urea is the precursor of Nitrogen, 1 and 3W%) is added drop wise to the mixed solution. Now the solution transforms to gel. After, aging 24 hours the gel is filtered and dried. The TiO_2 we get is then powdered and is used for further characterizations.

3. Material Characterization:

The prepared samples are characterized by Powder X-ray diffraction using XPERT PRO powder X-ray diffractometer. In the present study, FTIR spectra are recorded with Jasco 4100 model spectro photometer equipped with ATR. The UV-Vis absorption spectra are recorded using SHIMADZU UV-Vis spectrophotometer.

4. Results and Discussion:

4.1 PXRD Analysis:

The crystalline phase of the TiO_2 nanocrystals is identified using the most common technique powder X-ray diffraction [14]. The X-ray diffraction patterns are recorded in the range between 10 and 80˚. Figure (i) shows the PXRD spectrum of 1 and 3W% N-doped TiO_2 Nanocrystals. The figure confirms the presence of anatase crystalline phase and is good agreement with standard JCPDS (JCPDS file no. 21-1272) of an anatase crystalline phase [15]. The peaks are indexed accordance with the anatase tetragonal structure. The broad diffraction peak in the N-doped TiO_2 is also observed which is attributed to the decrease in the particle size [16]. Moreover, N-doping leads to the advantage of replacement of oxygen ions into nitrogen ions in the TiO_2 crystal lattice [17]. It is noted that there is no additional peak is detected related to the dopant. Hence, it is expected nitrogen ions merge into the interstitial positions or the substitutional sites of the TiO_2 crystal structure [16]. Crystallite size of TiO_2 nanocrystals are found from full width half maximum value of the (1 0 1) peak using the Scherrer formula $D=K\lambda/\beta \cos\theta$, where D is the crystallite size, λ is the wavelength of X-ray radiation (Cu Kα-1radiation= 1.54060 Å), K is a constant and is taken as 0.9, β is the full width at half maximum, θ is the half of the diffraction angle [18]. The estimated crystallite size is 11 and 13 nm for 1 and 3W% N-doped TiO_2 Nanocrystals, respectively.

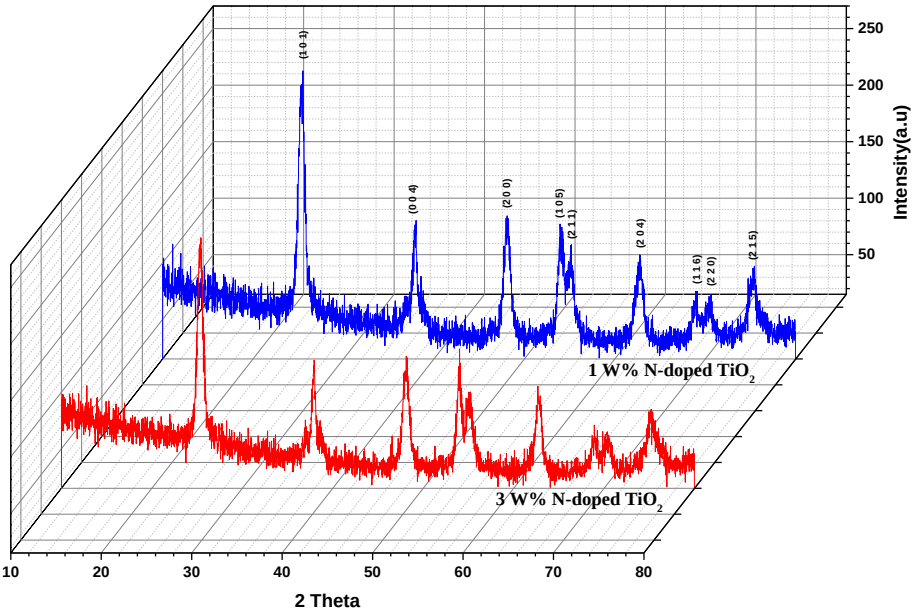

Figure (i): PXRD spectrum of 1 and 3W% N-doped TiO_2 Nanocrystals

4.2 FTIR Analysis:

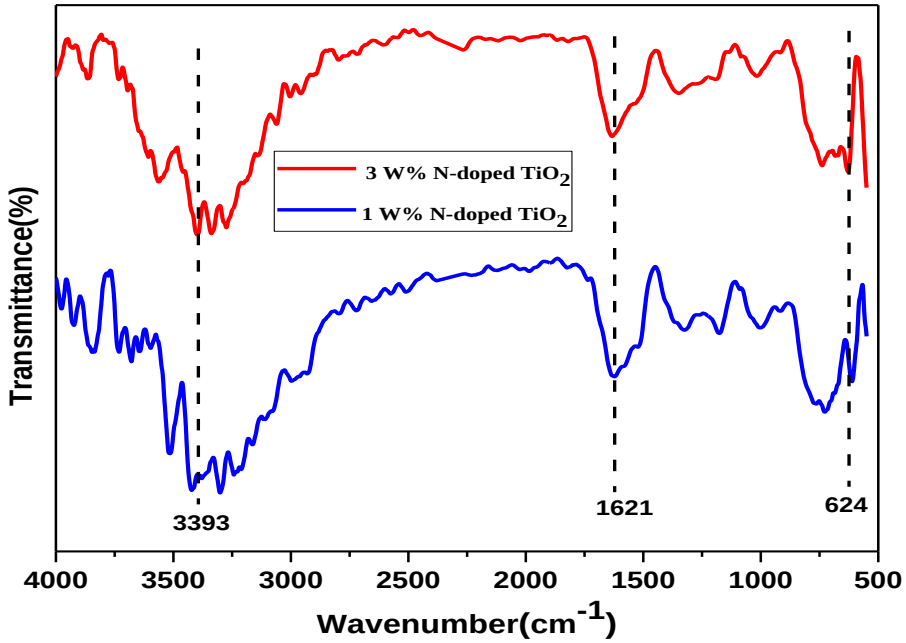

Figure (ii): FTIR spectra of 1 and 3W% of N-doped TiO_2 Nanocrystals

Figure (ii) shows the FTIR spectra of 1 and 3W% of N-doped TiO_2 nanocrystals.The vibrational peak observed around 3393 cm^{-1} attributed to the characteristic stretching mode of N-H bond, which confirms the successful doping of nitrogen into the TiO_2 crystal lattice [19]. Another strong vibration observed in the region around 1621 cm^{-1} corresponds to characteristic bending vibrations of O-H bond. The very strong peak observed in the range 500-650 cm^{-1} assigned to vibrations of Ti-O bond [20]. Other smaller peaks are vibrations of residual organic compounds which exist due to the effect of precursors.

4.3 UV-Vis Spectral Analysis:

The optical properties of N-doped TiO_2 nanocrystals are investigated by recording UV-Vis absorption spectra. In general, the optical band gap of TiO_2 nanocrystals is evaluated by using the Tauc's familiar formula,

$$(\alpha h\nu)^{\frac{1}{n}} = A\,(h\nu - E_g)$$

where α is the absorption coefficient of the material, E_g is the optical bandgap, A is a proportionality constant, hv is the energy of the photon, and n is a power factor which depends on nature of transition and is equal to 2 for indirect and 1/2 for direct band gap semi conductors [21]. Anatase phase TiO_2 is an indirect band gap semiconductor [22]. By plotting the graph between $(\alpha hv)^{1/2}$ and photon energy (hv) from UV-Vis absorption spectra, the band gap energy E_g of the N-doped TiO_2 nanocrystals are obtained by extrapolation of the linear portion of higher photon energy to zero absorption coefficient (α=0). The Tauc plot for 1 and 3W% N-doped TiO_2 nanocrystals is shown in figure (iii). The band gap values obtained from Tauc plot is 3.08 and 3.11 eV, which agrees well with the previously reported values [23].

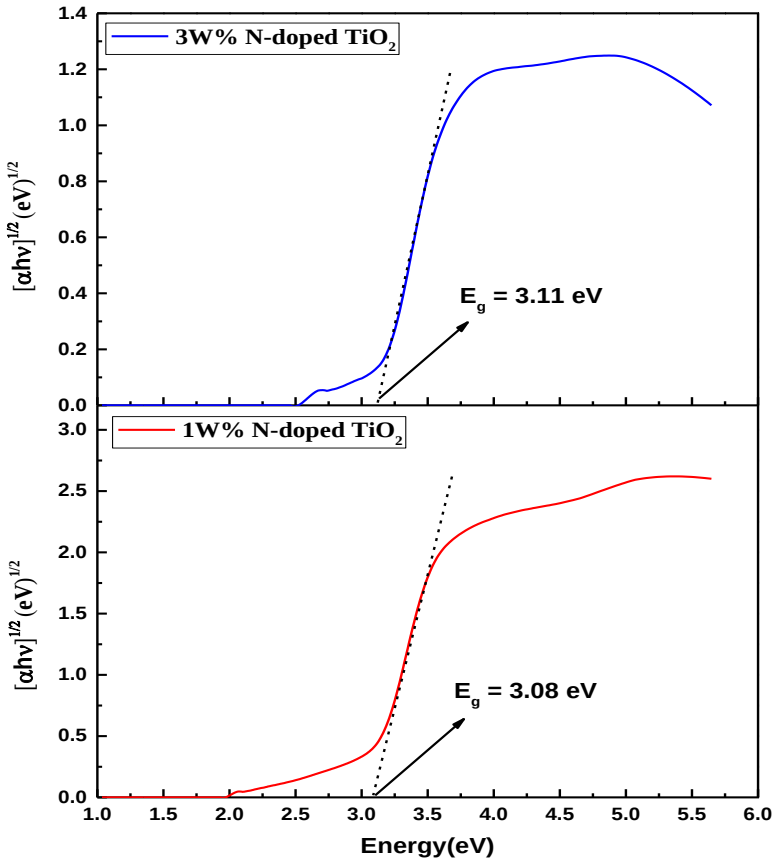

Figure (iii): Tauc plot of 1 and 3W% of N-doped TiO_2 Nanocrystals

5. Conclusions:

N-doped TiO_2 nanocrystals have been synthesized using the Sol-Gel method. The anatase phase of N-doped TiO_2 nanocrystals is confirmed by powder X-ray diffraction (PXRD). Broadening of peaks confirms that the size of the crystals is smaller in size. The FTIR spectroscopic study of the TiO_2 nanocrystals confirms the vibration of N-H bond around 3393 $cm^{-1}$and Ti-O bond around 624 cm^{-1}. The optical analysis suggests that the bandgap values are lowered on comparing to bulk TiO_2. Thus, one could conclude that the nitrogen doping with TiO_2 leads to band gap lowering towards the visible region, which is highly applicable for visible light photo catalysis.

6. References:

1. Fujishima, K. Hashimoto, T. Watanabe, TiO_2 photocatalysis, Fundamental and Applications, Bkc Inc., Tokyo, 1999.
2. J. Winkler, Titanium Oxide, Vincentz, Hannover, 2003.
3. A. Bozzi, T. Yuranova, J. Kiwi, J. Photochem. Photobiol. A, 108 (1997) 1–16.
4. W.S. Tung, W.A. Daoud, Acta Biomater, 172 (2005) 27–34.
5. D. Gumy, C. Morais, P. Bowen, C. Pulgarin, S. Giraldo, R. Hajdu, J. Kiwi, Appl. Catal. B, 63 (2006) 76–84.
6. V. Nadtochenko, N. Denisov, O. Sarkisov, D. Gumy, C. Pulgarin, J. Kiwi, J. Photochem. Photobiology A, 181 (2006) 401–407.
7. M.R. Hoffmann, S.T. Martin, W. Choi, D.W. Bahnemann, Chem. Rev., 95 (1995) 69.
8. C.S. Turchi, D.F. Ollis, J. Catal., 122 (1990) 178.
9. R.W. Matthews, J. Catal., 111 (1998) 264.
10. A.J. Nozik, Annu. Rev. Phys. Chem., 29 (1978) 189.
11. E. Pelizzetti, Sol. Energy Mater. Sol. Cells., 38 (1995) 453.

12. A.V. Taborda, M.A. Brusa, M.A. Grela, Appl. Catal. A Gen., 208 (2001) 419.
13. X. Chen, S.S. Mao, Chem. Rev., 107 (2007) 2891.
14. S. Sagadevan, J Material Sci Eng., (2015) 4:164.
15. S. S. Mandal, A.J. Bhattacgarya, Journal of Chemical Science. 124 (2012) 969-978.
16. X. Cheng, X. Yu, Z. Xing, J. Wan, Energy Procedia, 16 (2012) 598 – 605.
17. G. Barolo, S. Livraghi, M. Chiesa, M. C. Paganini, E. Giamello, J. Phys. Chem. C 2012, 116, 20887−20894.
18. S. Perumal, K. M. Prabu, C. Gnanasambandam, A. P. Mohamed, IJERA, (2014) 184-187.
19. M. Factorovich, L. Guz, R. Candal, Advances in Physical Chemistry, (2011) 821204.
20. T. Ivanova, A. Harizanova, M. Surtchev, Materials Letters, 55(2002) 327-333.
21. P.G. Wu, C.H. Ma, J.K. Shang, Applied Physics A –Materials Science & Processing, 2005, 1411–1417.
22. Y. Mi, Y. Weng, Scientific Reports, (2015) 11482 (10pp).
23. A. Zane, R. Zuo, F.A Villamena, A. Rockenbauer, A.M. Digeorge, Foushee, K. Flores, P.K. Dutta, A. Nagy, International Journal of Nanomedicine,11 (2016) 6459–6470.

.